Published in "Plant, Cell & Environment doi: 10.1111/pce.12397, 2014"
which should be cited to refer to this work.

The auxin response factor, OsARF19, controls rice leaf angles through positively regulating *OsGH3-5* and *OsBRI1*

SaiNa Zhang[1]*, SuiKang Wang[1]*, YanXia Xu[1], ChenLiang Yu[1], ChenJia Shen[1], Qian Qian[2], Markus Geisler[3], De An Jiang[1] & YanHua Qi[1]

[1]*State Key Laboratory of Plant Physiology and Biochemistry, College of Life Sciences, Zhejiang University, Hangzhou 310058, China,* [2]*State Key Laboratory of Rice Biology, China National Rice Research Institute, Chinese Academy of Agricultural Sciences, Hangzhou 310006, China and* [3]*Department of Biology – Plant Biology, University of Fribourg, Rue Albert-Gockel 3, Fribourg CH-1700, Switzerland*

ABSTRACT

Auxin and brassinosteroid (BR) are important phytohormones for controlling lamina inclination implicated in plant architecture and grain yield. But the molecular mechanism of auxin and BR crosstalk for regulating lamina inclination remains unknown. Auxin response factors (ARFs) control various aspects of plant growth and development. We here report that *OsARF19*-overexpression rice lines show an enlarged lamina inclination due to increase of its adaxial cell division. *OsARF19* is expressed in various organs including lamina joint and strongly induced by auxin and BR. Chromatin immunoprecipitation (ChIP) and yeast one-hybrid assays demonstrate that OsARF19 binds to the promoter of *OsGH3-5* and brassinosteroid insensitive 1 (*OsBRI1*) directing their expression. OsGH3-5-overexpression lines show a similar phenotype as *OsARF19-O1*. Free auxin contents in the lamina joint of *OsGH3-5-O1* or *OsARF19-O1* are reduced. OsGH3-5 is localized at the endoplasmic retieulum (ER) matching reduction of the free auxin contents in *OsGH3-5-O1*. *osarf19*-TDNA and *osgh3-5*-Tos17 mutants without erected leaves show a function redundancy with other members of their gene family. *OsARF19*-overexpression lines are sensitive to exogenous BR treatment and alter the expressions of genes related to BR signalling. These findings provide novel insights into auxin and BR signalling, and might have significant implications for improving plant architecture of monocot crops.

Key-words: *OsARF19*; *OsBRI1*; rice (*Oryza sativa* L.).

INTRODUCTION

Leaf angle (lamina inclination or lamina joint bending) is the degree of bending between the leaf blade and leaf sheath or the inclination between leaf blade and culm. Leaf angle is an important agronomic trait for determining plant architecture and grain yield. The regulatory mechanism of rice leaf angle depends on the coordination of several phytohormone signals including brassinosteroids (BRs) and auxin, which may be related to differential cell elongation by adaxial and abaxial cells in the lamina joint (Yokota & Mori 1992; Sakamoto *et al*. 2013). A conserved mechanism of BR regulation of plant development in *Arabidopsis* and rice acts through a pair of antagonizing HLH/bHLH (basic helix-loop-helix factors) transcription factors that act downstream of Brassinazole-resistant 1 (*BZR1*, Zhang *et al*. 2009a,b). OsGRAS19, a new member of the GRAS family [GA INSENSITIVE (GAI), REPRESSOR OF GAI (RGA) and SCARECROW (SCR)], is involved in the BR signalling pathway. OsGRAS19-overexpressing plants displayed larger leaf angles (Chen *et al*. 2013). However, *LC2* (*Leaf Inclination2*) controls leaf angles by inhibiting the adaxial cell division (Zhao *et al*. 2010); *ILA1* (*Increased Leaf Angle1*) affects leaf angles by regulating vascular bundle formation and cell wall composition in the leaf lamina joint (Ning *et al*. 2011), which is distinct from BR-dependent pathways. In a recent report, *Loose Plant Architecture 1* (*LPA1*), the functional rice ortholog of *AtIDD15*/*SHOOT GRAVITROPISM 5* (*SGR5*), was shown to regulate the leaf angle by controlling the adaxial growth of lamina joint, demonstrating the complicated nature of the rice leaf angle regulatory mechanism (Wu *et al*. 2013).

Besides the above recent reports, auxin was also shown to control normal leaf development in various aspects (Davies 1995). Wada *et al*. (1981) discovered that auxin has an impact on lamina inclination. Auxin early response genes, such as *AUX/IAA* and *GH3*, the auxin receptor TIR1, and auxin response factor (ARF), were reported in succession related to regulating leaf angle. Overexpression of OsIAA1 increased lamina joint angle and dwarfism (Song *et al*. 2009). In overexpressing lines of *MiR393a/b* and related *OsAFB2*- or *OsTIR1*-suppressed lines, flag leaf inclination was enlarged (Bian *et al*. 2012). Interestingly, OsTIR1 and OsAFB2 were shown to interact with OsIAA1 by using yeast two-hybrid and bimolecular fluorescence complementation assays (Bian *et al*. 2012). The auxin early response gene *GH3* encodes an indole-3-acetic acid-amido synthetase and functions in maintaining the auxin homeostasis through conjugating excess IAA to

Correspondence: Y. Qi. Fax: +86 571 88981355; e-mail: qyhjp@zju.edu.cn

*These authors contributed equally to this work.

various amino acids (Hagen & Guilfoyle 1985; Staswick *et al*. 2002). A gain-of-function rice mutant, *tld1-D* (*OsGH3-13*), displays an increased number of tillers, enlarged leaf angles, and dwarfism (Zhang *et al*. 2009a,b). The rice gain-of-function mutant, *lc1-D* (*Leaf inclination1*, alias *OsGH3-1*), and overexpressing lines of *OsGH3-1* all show enlarged leaf angles due to stimulated cell elongation at the lamina joints (Zhao *et al*. 2013). The other *OsGH3* gene family member, *OsGH3-2*, also acts in leaf inclination (Du *et al*. 2012). Increased leaf angle was observed in the *OsGH3-2* overexpressing rice lines. These reports showed that auxin homeostasis also has a crucial role in leaf inclination control. In a recent report, a loss-of-function mutant of *auxin response factor 11* (*OsARF11*) in rice, *osarf11-1*, showed a reduction in plant height and the leaf angle of flag leaves compared with wild type (WT) (Sakamoto *et al*. 2013). Furthermore, in the *osarf11-1* mutant, expression of *OsBRI1*, *OsIAA1*, *OsSAUR13* and *OsGH3-1* was decreased about 70% of WT rice, suggesting that OsARF11, even multiple OsARF proteins, may function in the transcription regulation of these genes.

ARFs are important for normal growth and development in plants. In *Arabidopsis*, they control tissue and organ development in four aspects. (1) Lateral root (LR) initiation (Okushima *et al*. 2005, 2007; Wilmoth *et al*. 2005; Fan *et al*. 2012): ARF7 and ARF19 regulate LR formation via direct activation of lateral organ boundary domains *(LBD)16* and *LBD29*. (2) Leaf development: ARF5/MONOPTEROS (MP) is critical to leaf initiation and vein pattern formation (Garrett *et al*. 2012). (3) Floral organ formation: *Arabidopsis* ARF6 and ARF8 regulate floral organ development via repression of class 1 knox genes (Tabata *et al*. 2010). (4) ARF10 affects shoot regeneration (Qiao *et al*. 2012). While a lot of ARFs have been investigated in the dicot, *Arabidopsis*, comparatively less is known in monocots such as rice. Besides the above-mentioned OsARF11 implicated in the regulation of leaf angle, functions of OsARF1, OsARF12 and OsARF16 have been investigated. OsARF1 functions in regulating the crown root (adventitious root, AR) formation via binding to the promoter of the *LBD* gene, *OsCRL1* (Waller *et al*. 2002; Inukai *et al*. 2005; Attia *et al*. 2009). OsARF12 acts in regulating root elongation, affecting iron accumulation and phosphate homeostasis (Qi *et al*. 2012; Wang *et al*. 2014). OsARF16 participates in phosphate starvation response (Shen *et al*. 2013). Here, we explore the biological functions of OsARF19, which works in controlling leaf angle trough *OsGH3-5* and *OsBRI1*.

MATERIALS AND METHODS

Plant materials and growth conditions

Rice plants (*Oryza sativa* L.) were grown in standard culture solution (Wang *et al*. 2009) in a greenhouse with a light/dark cycle of 12/12 h at 30/24 °C. *Nicotiana benthamiana* plants were grown on vermiculite containing Murashige and Skoog salt (MS) nutritional liquid in a growth chamber (light/dark cycle of 12/12 h at 25/18 °C). Six-week-old *N. benthamiana* plants were used for transient *Agrobacterium tumefaciens*-mediated expression.

Overexpression of *OsARF19* and *OsGH3-5* in *Nipponbare* (NIP)

The open reading frame (ORF) of *OsARF19* and *OsGH3-5* was amplified using the primers OVARF19U/L and OVGH3-5U/L shown in Supporting Information Tables S2 and S3, respectively. OsARF19 PCR products were cloned into pCAMBIA1300 containing a CaMV35S promoter to create an OsARF19-overexpression construct, 35S:OsARF19, while OsGH3-5 PCR products were recombined in the pH7FWG2 vector to create 35S:OsGH3-5:GFP vector. The two vectors above were introduced into *A. tumefaciens* strain EHA105 using electroporation and transformed into WT rice NIP (Hiei *et al*. 1994). Overexpression analysis of *OsARF19* and *OsGH3-5* genes was monitored by RT-PCR using the primers RTARF19U/L and OsGH3-5-qRT-U/L as listed in Supporting Information Tables S2 and S3, respectively.

Identification of *osarf 19* and *osgh3*-5 mutants

The identification of T-DNA insertion sites in the mutant *osarf19* (PFG-1B-11635.R) was carried out according to http://signal.salk.edu/cgi-bin/RiceGE. Right border primer Ngus-RB was used to confirm integration of T-DNA in *osarf19* and the gene-specific primers arf19U/L were used to identify WT band of *OsARF19*. The homozygous lines of the TOS17 insertion line for *OsGH3-5*, *osgh3-5* (NC0973), were identified by PCR using primer TOS17-tail16 to confirm the integration of TOS17 in mutant lines and gene-specific primers GH3-5-LP/RP to identify the corresponding WT band. The PCR insertion products were ligated with pUCm-T vector (Sangon, Shanghai, China) and transformed into *Escherichia coli* DH5α, and the flanking sequences of the T-DNA insertion site were sequenced (Sangon). To confirm the transcription level of the *OsARF19* and *OsGH3-5* genes in NIP, *osarf19 and osgh3-5* mutant, RT-PCR was performed using the primers RTARF19U/L and OsGH3-5-qRT-U/L as listed in Supporting Information Tables S2 and S3, respectively. Primer sequences for the PCR and RT-PCR are listed in Supporting Information Tables S2 and S3.

β-glucuronidase (GUS) staining

Construction of *OsARF19* and *OsGH3-5* promoter-β-glucuronidase (*OsARF19pro:GUS* and *OsGH3-5pro:GUS*) transgenic rice and GUS staining of seedlings were performed as described by Qi *et al*. (2012). The construction of *OsARF19* and *OsGH3-5pro:GUS* was performed according to a published method (Cheng *et al*. 2007). Primers ProARF19U/L in Supporting Information Table S2 and ProGH3-5-GUSU/L in Supporting Information Table S4 were used for amplification of the promoter region. *OsARF19pro:GUS* and *OsGH3-5pro:GUS* were introduced into the *A. tumefaciens* strain EHA105 and transformed into

NIP. The *DR5:GUS* auxin reporter described by Ulmasov *et al.* (1997a,b) was transformed into NIP, *OsARF19-O1*, *OsARF19-O2*, Dongjin (DJ) and *osarf19* for detecting auxin distribution.

Quantitative RT-PCR (qRT-PCR) analysis

Total RNA was isolated from leaves or roots of 14-day-old seedlings with various treatments. RNA extraction, reverse transcription and qRT-PCR were according to Wang *et al.* (2010). The sequence of the related primers for qRT-PCR is listed in Supporting Information Tables S2 and S7.

Measurement of IAA contents

The IAA concentrations of lamina joints in NIP, *OsARF19*-overexpression lines, *OsGH3-5*-overexpression lines, DJ and *osarf19* plants were measured by gas chromatography-selected reaction monitoring mass spectrometry (GC-MS), as described by Ljung *et al.* (2005). Germinated seeds were grown in standard culture solution for 7 d. About 0.5-cm-long lamina joint was excised. Furthermore, five independent biological replicates of each 20 mg sample were purified after addition of 250 pg of ^{13}C6-IAA internal standard using ProElu C18 (www.dikma.com.cn), and auxin contents were measured with FOCUS GC-DSQII (Thermo Fisher Scientific Inc, Waltham, MA, USA). For auxin influx measurement, the germinated seeds of NIP, *OsARF19-O1* and *OsARF19-O2* were grown in normal culture solution for 7 d.

Scanning electron microscopy

Scanning electron microscopy was conducted as described previously (Zhao *et al.* 2010). About 1-cm-long lamina joints of the third leaf from 2-month-old plant were excised from NIP and *OsARF19-O1* plants. Samples were observed with an S-3000N scanning electron microscope (Hitachi, Tokyo, Japan).

Microscopy of cross and longitudinal sections

Lamina joints (from flag leaf of 3-month-old NIP and *OsARF19-O1* plants) were collected for cross and longitudinal sections. Microscopic analysis was performed as described elsewhere (Qi *et al.* 2012). Ten independent sections were microscopically examined and photographed to measure the cell layers and cell lengths (Zhao *et al.* 2010).

ChIP-PCR analysis

Rice (NIP) protoplasts with transiently expressed *35S:OsARF19-GFP* were performed for ChIP-PCR assay as described in Du *et al.* (2009) and Zhang *et al.* (2011). The ChIP-IT® Express kit was used for target DNA enrichment according to the manufacturer's description (Active Motif, Carlsbad, CA, USA). The related primers in PCR of targets DNA are listed in Supporting Information Table S4.

Yeast one-hybrid assay

Yeast one-hybrid assays were carried out using the MATCHMAKER One-Hybrid Library Construction and Screening Kit (Takara, Dalian, China) according to the manufacturer's manual. Full-length cDNA sequences of *OsARF19* were PCR amplified using the primers OsARF19-orf-ADU/L shown in Supporting Information Table S5. *OsGH3-5* and *OsBRI1* promoter fragments containing WT AuxRE or mutated AuxRE were obtained by DNA renaturation (primers shown in Supporting Information Table S5).

Cell wall isolation and cellulose measurement

Shoots from 1-month-old NIP, *OsARF19*-overexpression lines and *OsGH3-5*- overexpression lines were collected for cell wall isolation and cellulose measurement. The assays were conducted as described previously (Zhang *et al.* 2012).

Agrobacterium-mediated transfection of *N. benthamiana* leaves and polyethylene glycol-mediated transformation of rice protoplast

Full-length cDNA of *OsARF19* was ligated into the binary vector pCAMBIA1300 under the control CaMV35S promoter (35S) resulting in *35S:OsARF19* vector. The promoter region of *OsGH3-5* was ligated into the sGFP vector resulting in *OsGH3-5pro:sGFP*. The primer sequences of OVARF19U/L and GH3-5-sGFPU/L are listed in Supporting Information Table S6. The above vectors were introduced into the *A. tumefaciens* strain EHA105 using electroporation respectively. *Agrobacterium*-mediated infection of *N. benthamiana* was performed as described previously (Chen *et al.* 2008; Qi *et al.* 2012). After 2 d, the fluorescence was visualized under a Nikon microscope equipped with NIS-Elements Basic Research 3.0 software (http://www.nis-elements.com). For the subcellular localization of OsGH3-5, 35S:OsGH3-5:GFP vector was infected to *N. benthamiana* through *Agrobacterium*-mediated transfection, and was introduced into rice protoplast by polyethylene glycol-mediated transformation, by Qi and Chen, respectively (Chen *et al.* 2011; Qi *et al.* 2012).

BR sensitivity tests

The coleoptile elongation test was performed as described previously (Duan *et al.* 2006). Germinated seeds of NIP, *OsARF19-O1* and *OsARF19-O1-O2* were grown in standard culture solution with 0, 0.001, 0.01, 0.1 and 1 μM 24-eBL for 7 d under dark condition. Then coleoptile lengths were photographed and measured. Primary root (PR) inhibition analysis was carried out as described previously with slight modification (Zhang *et al.* 2012). Germinated seeds were grown in normal culture solution supplemented with various concentrations of 24-eBL for 1 week, and then the root length was measured. Leaf angles were measured after 8 d in a dark growth and 3 d incubation with various concentrations of 24-eBL as described in Zhang *et al.* (2012).

Accession numbers

Sequence data from this article can be found in the Rice Genome Annotation Project or GenBank under the following accession numbers: OsARF19, LOC_Os06g48950, AK103312; OsGH3-5, LOC_Os05g50890, AK071721; OsGH3-1, LOC_Os01g57610, OsGH3-2, LOC_Os01g55940, OsGH3-13, LOC_Os11g32520, OsIAA1, LOC_Os01g08320; OsARF23, LOC_Os11g32110; OsTIR1, LOC_Os05g05800; OsBRI1, LOC_Os01g52050; OsBZR1, LOC_Os07g39220; OsD2, LOC_Os01g10040; OsD11, LOC_Os04g39430; OsDWARF, LOC_Os03g40540; OsACTIN, LOC _Os03g50885.

RESULTS

Phenotypes of rice *OsARF19* gain and loss-of-function lines

From our previous work, it was known that OsARF19 is an active transcription factor interacting with many OsIAAs in the nucleus (Shen *et al.* 2010). To understand the biological function of OsARF19, we constructed 11 *OsARF19*-overexpression rice lines (Fig. 1a,b). Compared with WT/NIP, 9 of 11 *OsARF19*-overexpression lines revealed dwarfism, narrow leafs, thin seeds and enlarged leaf angles (Supporting Information Table S1a,b). T5 generations of *OsARF19-O1* and *OsARF19-O2* in the *OsARF19*-overexpression rice lines were further analysed in detail. The plant height of *OsARF19-O1* or *-O2* was lower than 30% of WT/NIP (Fig. 1c); the flag leaf width of *OsARF19-O1* or *-O2* was narrower than 20% of WT/NIP (Fig. 1d) and the grain breadth of *OsARF19-O1* or *OsARF19-O2* was thinner than 18% of WT/NIP (Fig. 1e). Further quantitative measurement showed that the flag leaf angle at the heading stage and the second/third leaf at the vegetative period were about 38–20° compared with the WT/NIP, which typically reveals almost 120° (Fig. 1f–h). These altered morphologies of *OsARF19-O1* and *-O2* suggested that *OsARF19* might act in rice growth and development. Especially, the enlarged leaf angle, which is an important agronomic trait, in respect to the rice yield, motivated us to study the *OsARF19* in depth.

To understand how OsARF19 controls rice growth and development, a T-DNA inserted mutant of *OsARF19* (*osarf19*) found to own an insertion in the eighth exon of *OsARF19* gene in WT/DJ was identified and analysed (Supporting Information Fig. S1c–f and Tables S1 & S2). Our analysis showed that *osarf19* did not simply show opposite phenotypes of *OsARF19-O1* mentioned. This is probably because there are 25 members in ARF family of rice, and OsARF19 belongs to one of class IIa subfamilies including nine highly homologous OsARFs (Wang *et al.* 2007). Therefore, the OsARF19 gene seems to share with other OsARFs a high degree of redundancy. Nonetheless, in *osarf19* mutant, the LR number was clearly decreased to 30% of the WT/DJ (Fig. 1f). The results are consistent with that of the *arf7/arf19* double mutant revealing fewer LRs in *Arabidopsis* (Okushima *et al.* 2005).

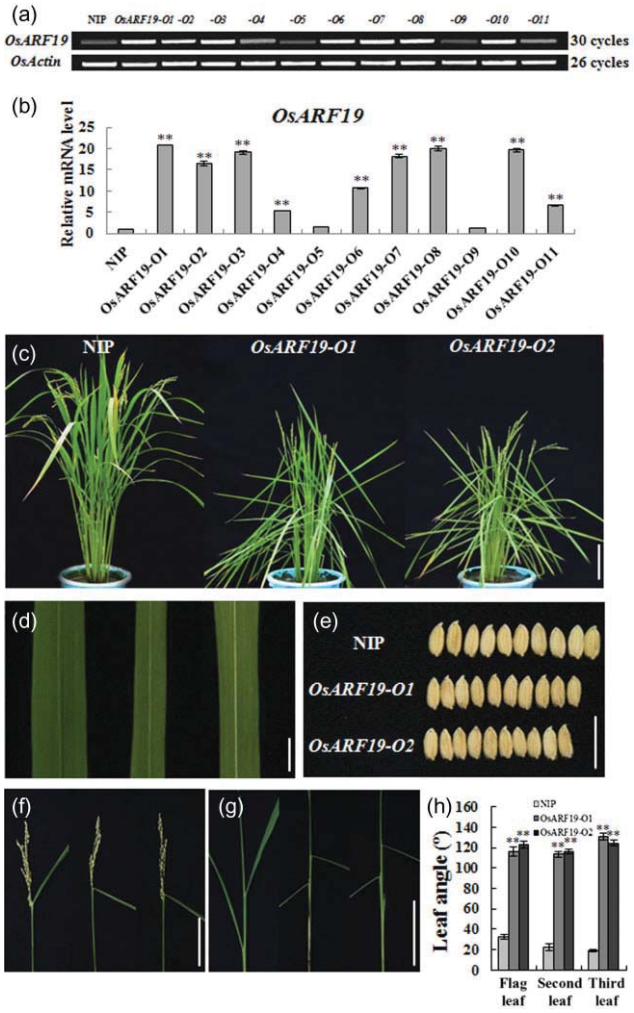

Figure 1. Phenotypes of *OsARF19*-overexpression lines. (a) *OsARF19* expression in NIP, *OsARF19*-overexpression lines using RT-PCR. (b) *OsARF19* expression in NIP, *OsARF19*-overexpression lines using qRT-PCR. Three independent biological replicates were used in the qRT-PCR analysis according to Wang *et al.* (2010). (c) Phenotypes of 3-month-old seedlings of NIP, *OsARF19-O1* and *OsARF19-O2* seedlings. Bar = 10 cm. (d) Leaf morphology of NIP, *OsARF19-O1* and *OsARF19-O2*. Bar = 1 cm. (e) Seeds of NIP, *OsARF19-O1* and *OsARF19-O2*. Bar = 1 cm. (f) Flag leaf angles at mature stages. Bar = 10 cm. (g) Leaf angles of second and third leaves at mature stages. Bar = 10 cm. (h) Leaf angles. Ten biological repeats were performed in each test. ** indicate significant difference at $P < 0.01$.

Osarf19-O1 shows increases of adaxial cell division at the lamina joint and reduction of cellulose contents

The lamina joint plays a significant role in leaf inclination formation and enlarged leaf inclination (Cao & Chen 1995; Yamamuro *et al.* 2000). To understand the involvement of OsARF19 in controlling rice leaf angle in the alteration of lamina joint, the collar length of lamina joint was measured. The collar lengths of adaxial surfaces in the lamina joint of *OsARF19-O1* and *OsARF19-O2* were increased by 60 and 55%, respectively, compared with the WT/NIP, while the

collar lengths in abaxial side were not significantly different from WT/NIP (Fig. 2a,b).

To clarify the cellular mechanism of OsARF19 controlling rice leaf angles, we further observed the microstructure of leaf lamina joint of rice WT/NIP and *OsARF19-O1*. Like in the *lc2* mutant, there is a bulge or cell protuberances in the adaxial surface of lamina joint, while *OsARF19-O1* has a smooth adaxial surface as in WT/NIP (Fig. 2c). The altered cell elongation and cell division in the lamina joint were therefore the two main reasons for the enlarged leaf angles (Duan *et al*. 2006; Zhao *et al*. 2010, 2013; Sakamoto *et al*. 2013). Observation of the cross and longitudinal sections revealed that the increased cell layers at the adaxial surface of the *OsARF19-O1* lamina joint were increased by about 45 and 60%, WT/NIP, respectively (Fig. 2e,h), illustrating that the enlarged leaf angle resulted from enhanced cell division but not cell elongation, that is, no alteration of cell size. In addition, the enlargement of cross sections showed that the vascular bundles in *OsARF19-O1* plant were smaller than those in the WT/NIP (under panel of Fig. 2d).

According to the microstructure characteristic of *OsARF19-O1* with smaller vascular bundles, we measured the cellulose content of the leaf in NIP, *OsARF19-O1* and *OsARF19-O2*. The cellulose contents in both *OsARF19*-overexpression lines were decreased about 30% compared with the WT/NIP (Fig. 2h). The result was similar with that of *ILA1*, which regulates leaf angle through altering vascular bundle formation and cell wall composition in the lamina joint (Ning *et al*. 2011).

OsARF19 is constitutively expressed in various organs including the lamina joint and is induced by auxin

To understand whether the OsARF19 functions in rice growth and development, we evaluated the expression patterns of *OsARF19* in various organs using the *GUS* reporter gene fusion. Ten positive transgenic lines were obtained and three lines were used for further investigation. GUS staining was found to be prominent in root including PR (or AR) and LR (Fig. 3a–c). *OsARF19* was expressed at a lower level in the leaf relative to shoot (Fig. 3d,e,i,l). *OsARF19* expression was also observed in the anther, stigma of the flower, glume, seed and lamina joint (Fig. 3f–h,j,k). qRT-PCR further confirmed that *OsARF19* was expressed at different levels in various tissues (Fig. 3l), consistent with the GUS staining results. Further, we found that *OsARF19* expression was induced by auxin treatments (Fig. 3m), suggesting that its function might be regulated by auxin. The expression pattern of OsARF19 matches well with the phenotypes of *OsARF19-O1* or *OsARF19-O2* mentioned above, further implying that OsARF19 may function in the various aspects of growth and development of rice organs and tissues.

OsARF19 binds to the *OsGH3-5* promoter and up-regulates *OsGH3-5* expression

In rice, the function of the three early auxin response genes, *OsGH3*-1, *OsGH3*-2 and *OsGH3*-13, was shown to result in increasing leaf angles (Zhang *et al*. 2009a,b; Du *et al*. 2012; Zhao *et al*. 2013). ARFs are transcription factors controlling OsGH3 gene expression such as the MicroRNA160-ARF17-GH3.2 (or GH3.3, GH3.5 and GH3.6) pathway in *Arabidopsis* (Mallory *et al*. 2005) and the MicroRNA167-ARF8-GH3.2 pathway in rice (Yang *et al*. 2006). To investigate whether these *OsGH3* genes are direct targets of OsARF19, sequence analysis of auxin response elements (AuxRE) of *OsGH3* promoters was performed, indicating that there were several AuxRE elements in the *OsGH3-2*, *-5* and *-13* promoters besides *OsGH3-1* (Supporting Information Fig. S2). Further, ChIP assays were carried out by transiently transforming 35S:OsARF19-sGFP into rice protoplast. The DNA elements pulled down by 35S:OsARF19-sGFP were enriched and analysed by PCR using three primers included in *OsGH3-1*, *-2*, *-5* and *-13* promoter elements, respectively (Fig. 4a and Supporting Information Table S4). Our experiments showed that the promoter regions of *OsGH3-2*, *-5* and *-13* were enriched in the ChIP assays with *OsGH3-5* being the most prominent. Furthermore, *OsGH3-1* was not enriched there, indicating *OsGH3-1* was not a direct target of OsARF19 but was indirectly induced by OsARF19 due to unknown mechanism.

To further confirm the binding of OsARF19 to the *OsGH3-5* promoter, we performed yeast one hybrid using *in vitro*-expressed OsARF19. As shown in Fig. 4b (Supporting Information Figs S2 & S5), OsARF19 bound to the AuxRE-containing DNA fragments (tgtctc) of *OsGH3-5* promoter but failed to bind AuxRE–mutated motifs (aaaaaa). The results further demonstrated OsARF19 as an upstream regulating factor of *OsGH3-5*, directly binding to the *OsGH3-5* promoter.

To demonstrate that OsARF19 controls rice leaf angles through *OsGH3* genes, the transcriptional level of several early auxin response *OsGH3* genes was quantified by qRT-PCR analysis (Fig. 4c). The transcripts of *OsGH3*-1, -2, -5 and -13 were all up-regulated in *OsARF19-O1* or *OsARF19-O2* compared with WT/NIP, while these OsGH3 genes were down-regulated in *osarf19* mutant compared with WT/DJ.

To test whether the binding of OsARF19 to the *OsGH3-5* promoter affects expression of the OsGH3-5 protein, the vectors of *35S:OsARF19-over* and *OsGH3-5pro:GFP* (green fluorescent protein) were co-transformed into leaves of *N. benthamiana* (Fig. 4d and Supporting Information Table S6). Fluorometric analysis of GFP showed that OsARF19 indeed significantly enhanced the fluorescence intensity of *OsGH3-5pro:GFP*. The result indicated that OsARF19 also promoted the expression of *OsGH3-5* on the protein level.

OsGH3-5-overexpression lines show similar phenotypes as *OsARF19-O1* or *OsARF19-O2*

In order to gain genetic information on the relationship between *OsARF19* and *OsGH3-5*, we constructed 12 *OsGH3-5*-overexpression rice lines (Supporting Information Fig. S3a,b). Ten of the *OsGH3-5*-overexpression lines in T3 generation revealed similar phenotypes with *OsARF19-O1*, characterized by enlarged leaf angles, dwarfism, narrow leafs

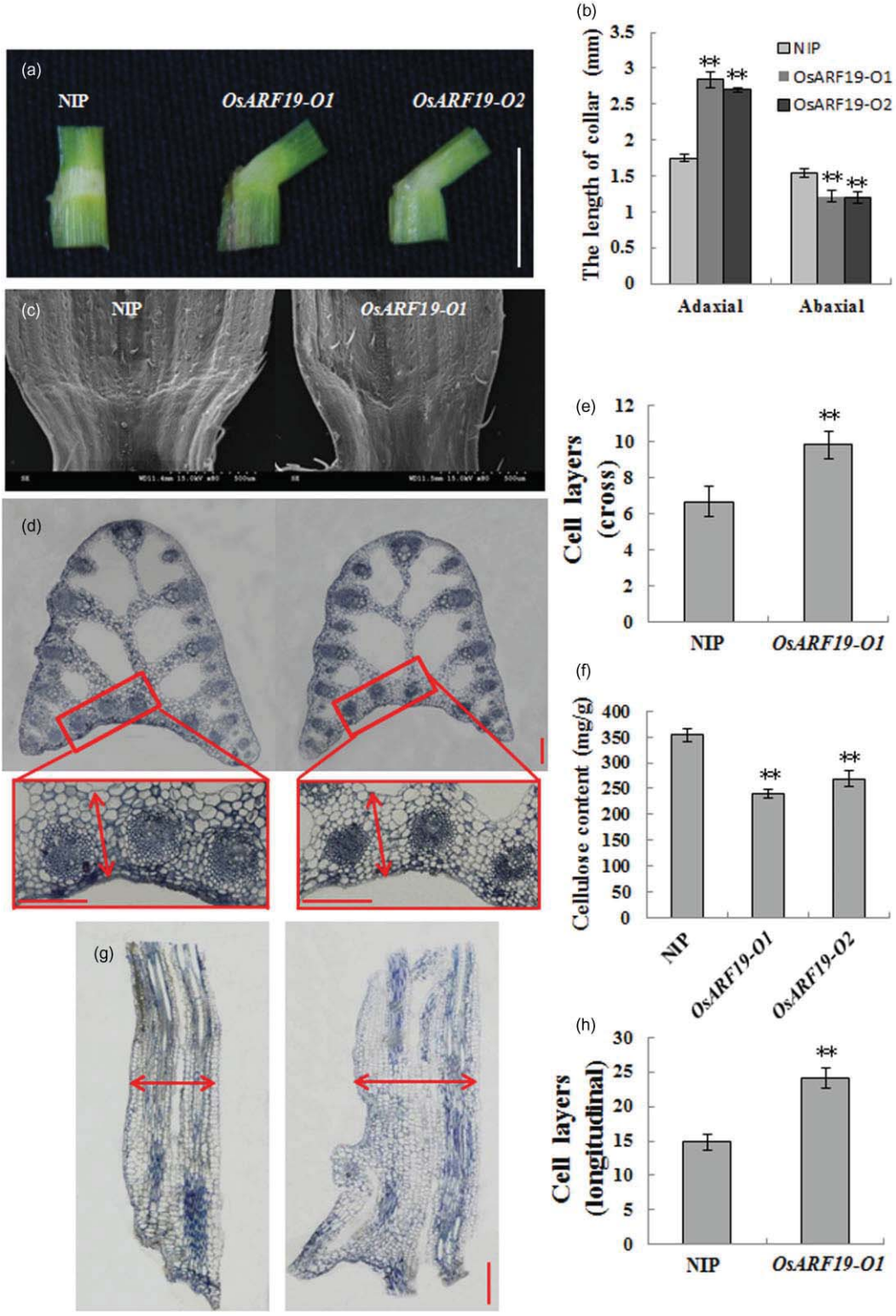

Figure 2. Microstructure analysis of lamina joints in WT/NIP, *OsARF19-O1* and *OsARF19-O2*. (a) Comparison of the lamina joint of flag leaves from 3-month-old seedlings of NIP, *OsARF19-O1* and *OsARF19-O2*. (b) Collar lengths of adaxial and abaxial surfaces of the flag leaves. (c) Scanning electron microscopy images of the adaxial surfaces in the lamina joint of the flag leaves. (d) Cross section of lamina joints of flag leaves in NIP and *OsARF19-O1*. Upper panel, 4 × amplification; lower panel, 10 × amplification. (e) Adaxial cell layers of cross sections. (f) Cellulose contents in WT/NIP, *OsARF19-O1* and *OsARF19-O2*. (g) Longitudinal section of lamina joint of the flag leaves in NIP and *OsARF19-O1*. (h) Cell layers of the longitudinal sections of lamina joints. Ten biological repeats were used for each test. Error bars indicate SD ($n = 10$). ** indicate significant difference at $P < 0.01$. Bars = 200 μm.

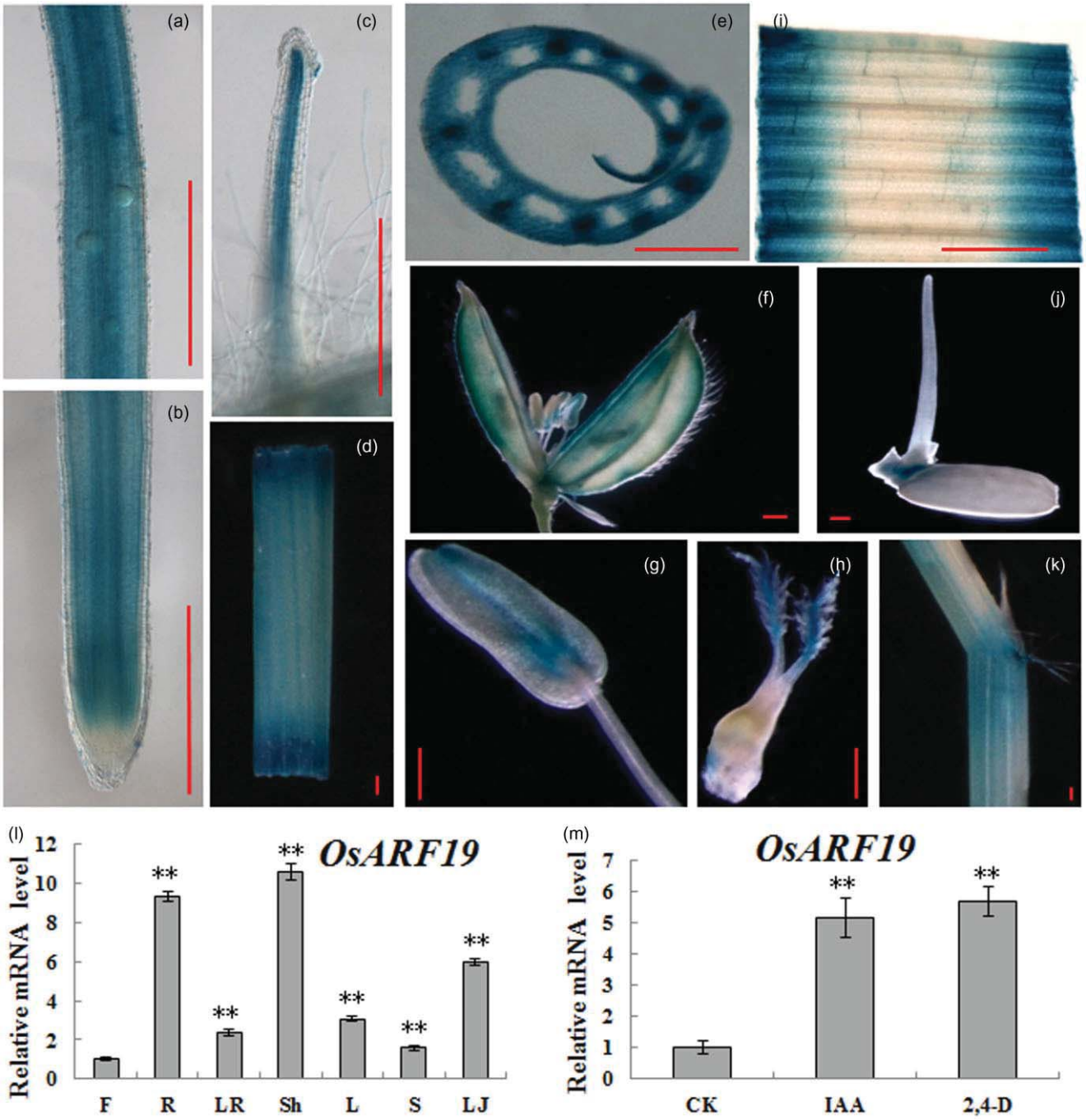

Figure 3. Expression patterns of the *OsARF19* gene. (a, b) Primary roots (expression pattern of *OsARF19* in adventitious roots was the same as in primary root). (a) Elongation region. (b) Meristem region to root cap. (c) Lateral root and root hair. (d) Shoot. (e) Cross section of leaf sheath. (f–h) Glume and flower. (f) Glume. (g) Anther. (h) Ovary and stigma. (i) Leaf. (j) Seed germinated for 3 d. (k) Lamina joint of top leaf of 1-month-old seedling. *OsARF19pro:GUS* was transformed into rice WT/NIP. Ten positive transgenic rice lines were used for analyses of GUS expression. A total of 7-day-old roots, shoots, leaves and other tissues were photographed. All bars = 400 μm. (l) qRT-PCR analysis of *OsARF19* expression in WT/NIP rice. L: leaf, F: flower, R: root, LR: lateral root, Sh: shoot, S: seed, LJ: lamina joint. *OsACTIN* gene was used as an internal reference. Three independent biological replicates were used in the experiments. Error bars indicate SD ($n = 3$). * indicates significant difference at $P < 0.05$ and ** indicates $P < 0.01$. (m) OsARF19 expression under auxin treatments. One-week-old WT/NIP seedlings were grown in solution containing 10 μM IAA and 1 μM 2,4-D for 3 h, respectively. qRT-PCR analysis was performed as described as in Fig. 3l.

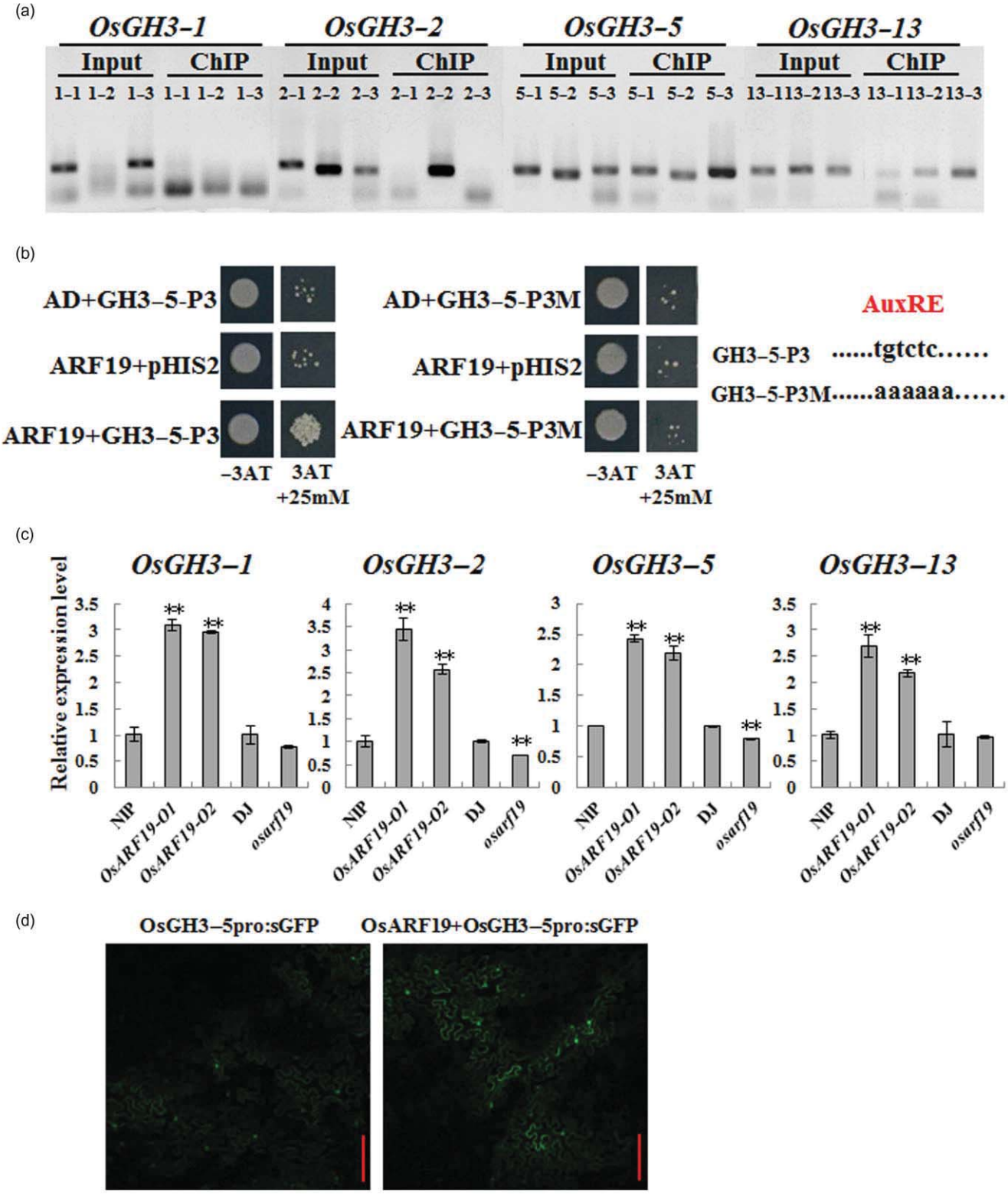

Figure 4. OsARF19 directly activates expression of *OsGH3-5*. (a) ChIP-PCR analysis. The ChIP of *OsARF19* assays was performed using rice *Nipponbare* protoplasts expressing the *35S:OsARF19-GFP* fusion. Products of ChIP assays were amplified using three specific primers (listed in Supporting Information Table S4) with the AuxRE elements in *OsGH3-2*, *-5* and *-13* promoters or without the AuxRE in *OsGH3-1* promoter, respectively. (b) Yeast one-hybrid (YOH) analysis of OsARF19 and *OsGH3-5* promoter. The bait vector containing the *OsGH3-5* promoter fragment P3 or the mutated P3 (P3M)-fused HIS2 reporter gene, and the prey vector containing OsARF19-fused GAL4 activation domain were co-transformed into yeast cells (Y187). Yeast cells were grown on (SD–Trp/–Leu/–His) media supplemented with 25 mM 3-amino-1, 2, 4-triazole (3AT) or without 3AT (-3AT) to suppress background growth or not. AD + GH3-5-P3/P3M and OsARF19 + pHIS2 were used as negative controls. The core region of P3 and P3M was indicated on the right. (c) Relative mRNA levels of *OsGH3* genes in the leaf lamina joints of WT/NIP, *OsARF19-O1*, *OsARF19-O2*, WT/DJ and *osarf19*. qRT-PCR analysis using three independent biological replicates was performed according to Wang *et al.* (2010). Error bars indicate SD ($n = 3$). ** indicates significant difference at $P < 0.01$. (d) *35S:OsARF19* and *OsGH3-5pro:sGFP* co-expression in *Nicotiana benthamiana*. *Agrobacterium*-mediated transient expression in leaves of *N. benthamiana*. Left panel shows *OsGH3-5pro:sGFP* expression for a negative control. Right panel shows co-expression of *35S:OsARF19* and *OsGH3-5pro:sGFP*. Bars = 50 μm.

and thin seeds (Fig. 5a and Supporting Information Fig. S3). For details, at heading stage, the flag leaf angle in *OsGH3-5-O1* or *-O2* was enlarged to 120° compared with that of WT/NIP showing 20° (Fig. 5b,c). To prove if the enlarged angles in *OsGH3-5*-overexpression lines impaired cellulose contents, cellulose contents were measured. The cellulose contents in *OsGH3-5-O1* or *-O2* were lower than 57% of WT/NIP (Fig. 5d). These results are consistent with those of *OsGH3-1*, *-2* or *-13* overexpression lines, which had exaggerated leaf angles (Zhang *et al*. 2009a,b; Du *et al*. 2012; Zhao *et al*. 2013). These phenotypes of *OsGH3-5*-overexpression rice lines further underline the genetic relationship of *OsARF19* being upstream of *OsGH3-5*.

So far, 13 members of the *OsGH3* gene family were cauterized in rice (Jain *et al*. 2006; Zhang *et al*. 2009a,b). Furthermore, the function of *OsGH3-1*, *-2* and *-13* acting in leaf angle regulation has been reported by using their overexpression transgenic lines (Zhang *et al*. 2009a,b; Du *et al*. 2012; Zhao *et al*. 2013). However, the mutants of the above *OsGH3* genes showed no obvious phenotype, suggesting the *OsGH3-5* and the above *OsGH3* genes share functional redundancy. To confirm this hypothesis, we analysed an *osgh3-5* mutant inserted with TOS17 in fourth exon (Supporting Information Fig. S4a and Table S3). The *OsGH3-5* gene was knocked out in the homozygous *osgh3-5* mutant (Supporting Information Fig. S4b–d). The leaf angle in the *osgh3-5* mutant was not different from WT/NIP (Supporting Information Fig. S4e,f); however, in the *osgh3-5* mutant, glumes were cracked and seed setting rate was very low (20% of WT) (Supporting Information Fig. S4g–i). These results imply that the function of *OsGH3-5* in regulating leaf angle is redundant with other *OsGH3* genes, but its function may be specialized in glumes development.

ER localization of OsGH3-5 matches a reduction of free auxin contents in *OsGH3-5-O1*

OsGH3 genes encode for IAA-amido synthetases conjugating excess IAA to various amino acids (Hagen & Guilfoyle 1985; Staswick *et al*. 2002). In *Arabidopsis*, the ER is thought to be an important compartment for auxin conjugation (Mravec *et al*. 2009). Using transient expression of *OsGH3-5* fused to a GFP in *N. benthamiana* and rice protoplast, the subcellular localization of *OsGH3-5* was demonstrated to be in the nucleus, cytoplasm and the ER (Fig. 6a–c).

In order to investigate further OsGH3-5 function, the expression pattern of *OsGH3-5* was also analysed. Both the experiments *OsGH3-5promoter:β-glucuronidase* (*GUS*) staining and qRT-PCR were examined (Supporting Information Fig. S5). As shown in Supporting Information Fig. S5, *OsGH3-5* is expressed in lamina joints and other tissues matching the expression pattern of *OsARF19* in Fig. 3. These tissue-specific expression patterns were consistent with the phenotypes of *OsGH3-5*-overexpression lines and *osgh3-5*. *OsGH3-5* expression in lamina joints was significantly induced by auxin treatments (Fig. 6d,e), indicating that OsGH3-5 was auxin responsive and thus regulated by auxin.

Furthermore, the auxin reporter *DR5:GUS* was expressed in WT/NIP and *OsGH3-5-O1*, respectively (Fig. 6f). *DR5:GUS* in *OsGH3-5-O1* was markedly shallower than in WT/NIP. Moreover, free auxin contents in lamina joints in WT/NIP, *OsGH3-5-O1* and *OsGH3-5-O2* were measured using GC-MS (Fig. 6g). The results also showed that the auxin contents in *OsGH3-5-O1* or *-O2* were lower than those in WT/NIP. These results imply that the OsGH3-5 might function in auxin conjugation.

OsARF19-O1 and *OsARF19-O2* show decreased free IAA contents at lamina joints

In order to explore if the transcription factor OsARF19 upstream of *OsGH3-5* affects the leaf angle through regulating free IAA contents, we analysed IAA contents and IAA distribution in the lamina joints of rice NIP, *OsARF19-O1*, *OsARF19-O2*, DJ and *osarf19* using GC-MS and *DR5:GUS* analyses, respectively (Fig. 7a,b). The results show that IAA contents in the lamina joint of *OsARF19-O1* or *-O2* were reduced to ~20% of WT/NIP, while in the *osarf19* mutant they were enhanced by ~20% compared with the WT/DJ. *DR5:GUS* staining in the lamina joint of *OsARF19-O1* or *-O2* was significantly weaker than that in WT/NIP, while in the *osarf19* mutant signals were stronger than in WT/DJ. Decreased IAA contents in *OsARF19-O1* or *-O2* were consistent with those in *OsGH3-5*-overexpression lines.

To further reveal the molecular mechanism of OsARF19 in controlling leaf angles, the expression of genes involved in leaf inclination and in auxin signalling was analysed in the lamina joints of rice NIP, *OsARF19-O1*, *OsARF19-O2*, DJ and *osarf19* (Fig. 7c). The transcript abundances of the genes *auxin/indole-3-acetic acid 1 (OsIAA1)* were induced in

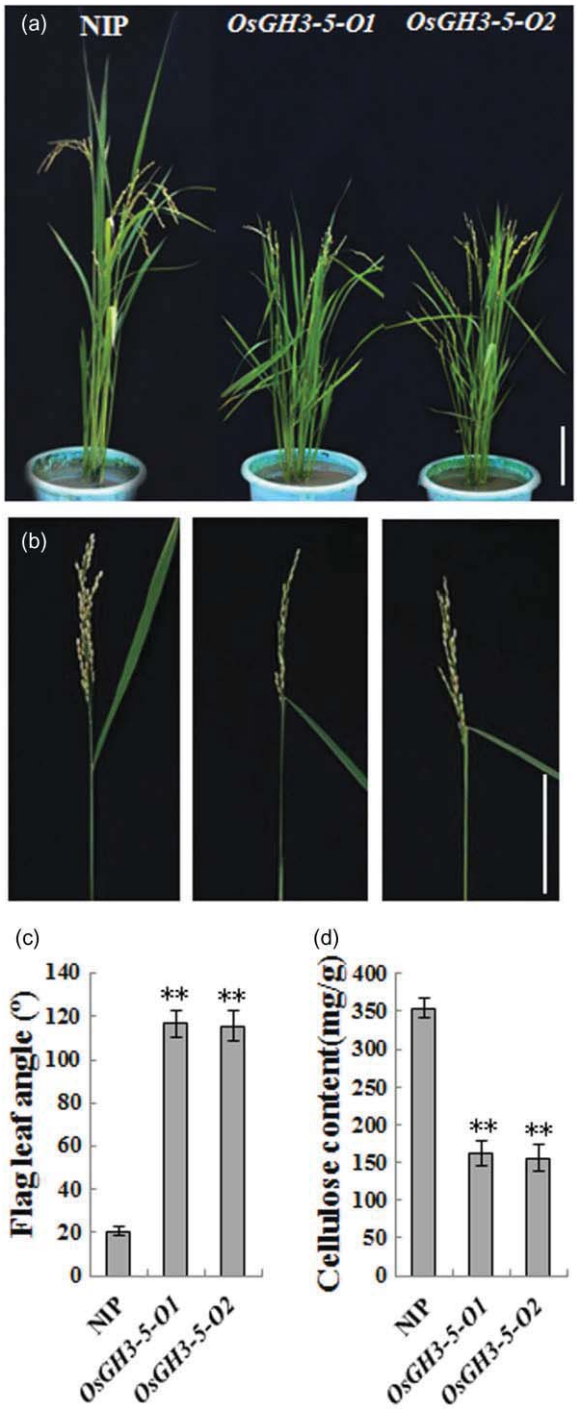

Figure 5. Characterization of *OsGH3-5*-overexpression lines. (a) Phenotypes for 3-month-old seedlings of NIP, *OsGH3-5-O1* and *OsGH3-5-O2*. (b) Leaf angles of NIP, *OsGH3-5-O1* and *OsGH3-5-O2*. Bar = 10 cm. (c) Statistical analyses of flag leaf angle. (d) Cellulose contents in WT/NIP, *OsGH3-5-O1* and *OsGH3-5-O2*. Ten biological replicates were used in each test. Error bars indicate SD ($n = 10$). ** indicates significant difference at $P < 0.01$.

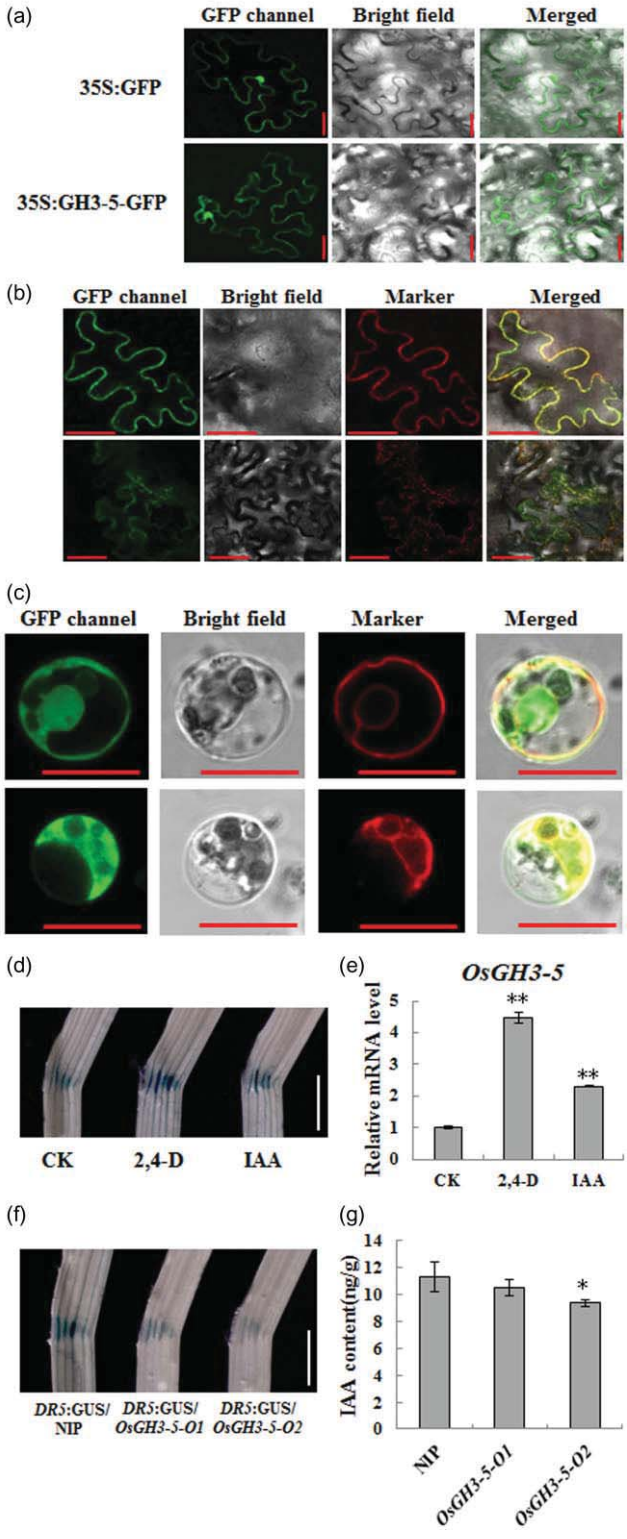

OsARF19-O1 or *-O2* compared with WT/NIP, while they were reduced in *osarf19*. Importantly, both genes, *OsARF23 (1)* and *transport inhibitor response 1* (*OsTIR1*), interacting with OsIAA1 showed opposite trends compared with

Figure 6. Subcellular localization of OsGH3-5, *OsGH3-5* induction by auxin and auxin contents in *OsGH3-5*-overexpression lines. (a) Subcellular localization of OsGH3-5 in *Nicotiana benthamiana* leaves transfected with *35S:GFP* and *35S:GH3-5-GFP*. (b) Co-localization of *35S:GH3-5-GFP* with plasma membrane marker, pm-rb CD3-1008 (upper panel), and ER marker, ER-rk CD3-960 (lower panel). (c) Co-transformation of rice protoplasts with *35S:GH3-5-GFP* and plasma membrane and ER marker as under (b). All bars = 50 μm. (d) *OsGH3-5promoter:GUS* analyses of lamina joints of 7-day-old WT/NIP after control (CK), 10 μM IAA and 1 μM 2,4-D treatments for 3 h, respectively. Each three transgenic rice lines were used for the experiments. (e) *OsGH3-5* expression in lamina joints of 7-day-old WT/NIP rice after CK, 10 μM IAA and 1 μM 2,4-D treatments for 3 h, respectively, analysed by qRT-PCR. (f) *DR5-GUS* analyses in lamina joints of WT/NIP, *OsGH3-5-O1* and *OsGH3-5-O2*. Each three transgenic rice lines were used in these experiments. (g) Auxin contents in lamina joints of 7-day-old WT/NIP, *OsGH3-5-O1* and *OsGH3-5-O2*. Three biological repeats were used in each test. Error bars indicate SD ($n = 3$) and one or two asterisks indicate significant difference at $P < 0.05$ and $P < 0.01$, respectively.

OsIAA1. Similarly, OsARF19 expression in OsTIR1-suppressed lines, *osafb2* or its upstream *OsMiRNA393-OVa* and *-OVb* was also up-regulated (Supporting Information Fig. S6), suggesting that both *OsARF19* and *OsTIR1* are negatively regulating each other. These results agree with those OsTIR1-suppressed transgenic rice lines and *OsIAA1*-overexpression transgenic rice lines, which exhibited increase of leaf inclination (Song *et al*. 2009; Bian *et al*. 2012).

OsARF19-overexpression lines are sensitive to exogenous BR and alter expression of BR response and biosynthesis genes

BR signalling plays an important role in controlling the leaf angle size (Yokota & Mori 1992; Sakamoto *et al*. 2013). To understand whether OsARF19 is involved in BR signalling, we first performed three classical BR sensitivity experiments including coleoptile elongation, root growth and degree of leaf inclination using various concentrations of 24-eBL treatments (Fig. 8). Comparison of coleoptile elongation between WT/NIP, *OsARF19-O1* and *OsARF19-O2* revealed that the elongated coleoptile length became more pronounced with the increased BR concentration (Fig. 8a,d). In contrast to coleoptile elongation, PR growth was inhibited by BR treatments (Fig. 8b,d). The PR length of *OsARF19-O1* or *-O2* was 12% shorter than that of WT/NIP in absence of BR, while it was shorter 38% than WT under 1 μM 24-eBL treatment. The lamina joint angle in *OsARF19-O1* or *-O2* showed also a significant increase by 8–30% compared with that of WT/NIP under various concentration of 24-eBL treatments (Fig. 8c,d). Taken together, the above data indicate that *OsARF19-O1* and *-O2* were more sensitive to BR than WT/NIP, suggesting that OsARF19 could be related to BR signalling.

Furthermore, ChIP-PCR assays and yeast one hybrid confirmed that OsARF19 binds to OsBRI1 promoter using three different primers (Supporting Information Fig. S7 and Tables S4 & S5). Furthermore, the expressions of genes controlling leaf angle on BR response and biosynthesis in WT/NIP, *OsARF19-O1*, were analysed by qRT-PCR under control and BR treatment condition (Fig. 8e). The expression of the BR response genes *OsBRI1* and *Brassinazole-resistant 1* (*OsBZR1*) in WT/NIP was lower than that in *OsARF19-O1* under control condition (Yamamuro *et al*. 2000; Bai *et al*. 2007). Furthermore, under BR treatment, their expression in WT/NIP and *OsARF19-O1* was all decreased. However, the decreased ranges in *OsARF19-O1* were higher than those in WT/NIP, further demonstrating that *OsARF19-O1* was sensitive to exogenous BR. Further, BR biosynthetic genes *OsD2 (CYP90D2)*, *OsDWARF (CYP85A4)* and *OsD11 (CYP724B1)* were all significantly up-regulated in *OsARF19-O1* than in WT/NIP under normal growth (control) condition (Hong *et al*. 2002, 2003; Tanabe *et al*. 2005). Furthermore, they were dramatically down-regulated in WT/NIP and *OsARF19-O1* under BR treatment compared with control condition, implying that these genes were modulated by OsARF19 under control condition but feedback-regulated by BR treatment. These results further confirmed that OsARF19 is involved in regulating BR signalling.

DISCUSSION

OsARF19 functions in regulating leaf angles through directly altering *OsGH3-5* expression

ARFs in *Arabidopsis* are involved in transcriptional control of several GH3 genes. Such ARF7 positively regulates the expression of the *GH3-2/YDK1* gene, which functions in hypocotyl and root elongation (Stowe-Evans *et al*. 1998; Takase *et al*. 2004); ARF8 binds to *AtGH3* promoters to regulate the expression of three *AtGH3* genes involved in the adenylation of IAA, which results in the formation of IAA amino acid conjugates (Tian *et al*. 2004); ARF17 increases *GH3-2/YDK1*, *GH3-3*, *GH3-5* and *DFL1/GH3-6* mRNA levels and leads to dramatic developmental tissue and organ defects (Mallory *et al*. 2005). In rice, the knowledge of the transcriptional control of genes involved in auxin homeostasis is still scarce. In this study, *OsARF19*-overexpression rice lines showed multiple phenotypes, including increased leaf angles, decreased height and reduced leaf width, suggesting that OsARF19 is critical in the regulation of rice architecture (Fig. 1). Our experimental data demonstrated the important role of OsARF19 in leaf inclination regulation through modulating adaxial cell division of the collar (Figs 2 & 3). We further uncovered that OsARF19 directly binds to the promoter of *OsGH3-5* using ChIP assay, and positively regulated OsGH3-5 expression (Fig. 4). Genetic phenotypes of *OsGH3-5*-overexpression lines and expression pattern of *OsGH3-5* further confirmed these results (Fig. 5 and Supporting Information Fig. S5). Previous reports and our results together indicate that ARF regulation of *GH3* genes is conserved between dicot and monocot. Our findings strongly support that OsARF19 functions in regulating leaf angles through directly altering *OsGH3-5* expression.

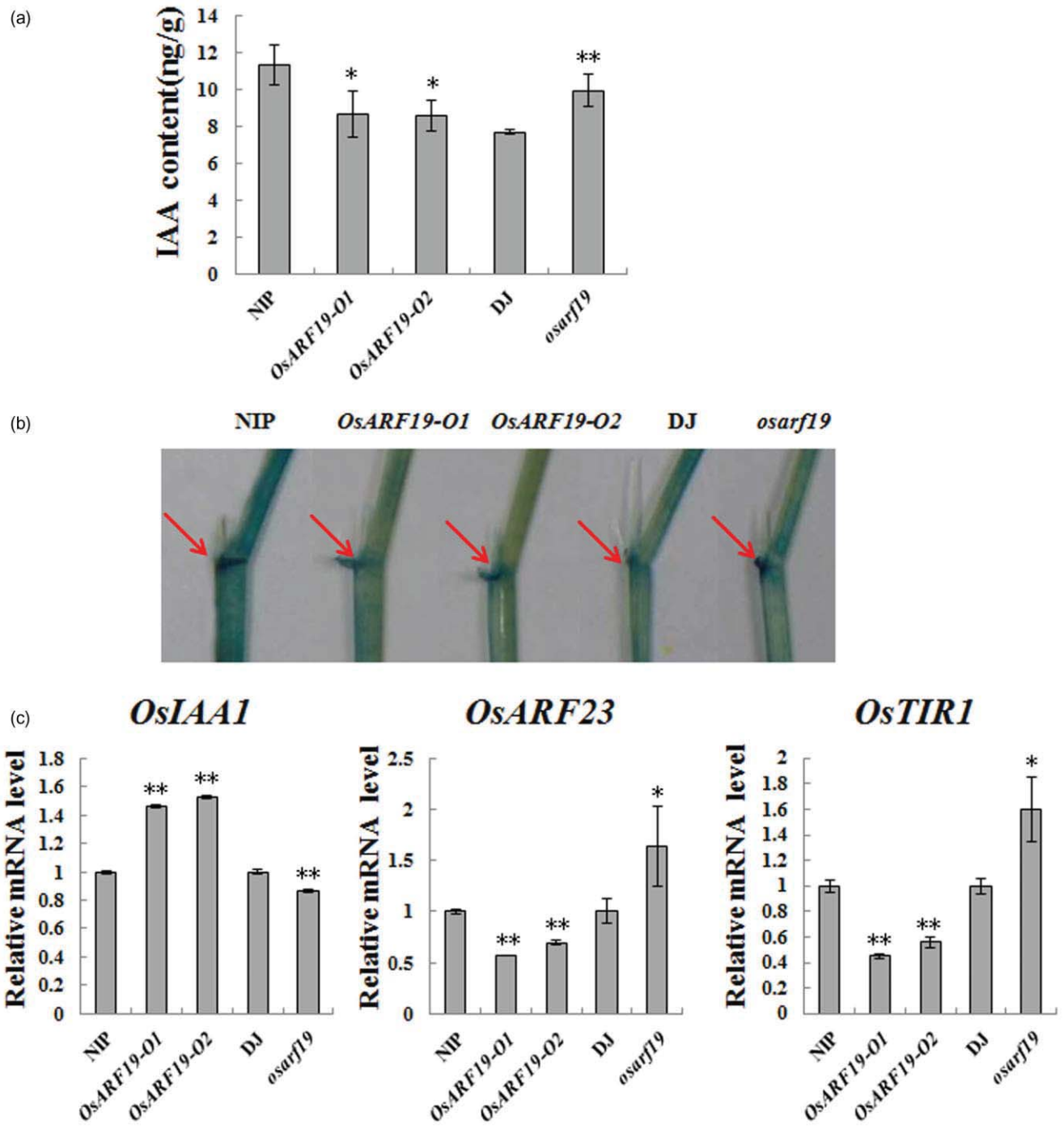

Figure 7. Auxin distribution at lamina joints and expression of genes implicated in the increase of leaf angles in auxin signalling. (a) Auxin contents in lamina joints of 7-day-old WT/NIP, *OsARF19-O1*, *OsARF19-O2*, WT/DJ and *osarf19*. (b) GUS staining in lamina joints of WT/NIP, *OsARF19-O1*, *OsARF19-O2*, WT/DJ and *osarf19* transformed with the auxin reporter, *DR5:GUS*. Each three transgenic rice lines were used in these experiments. (c) Expression of genes implicated in the increase of leaf angles in auxin signalling. Three biological repeats were used in the test. Error bars indicate SD ($n = 3$). * indicates significant difference at $P < 0.05$ and ** indicates $P < 0.01$.

Alteration of auxin level in the lamina joint might result in enlarged leaf angles

In rice, *OsGH3* genes were classed into two groups, group I and group II. *OsGH3-5* belongs to group I including *OsGH3-3*, *-5*, *-6* and *-12*, which show high homology to *AtGH3-10* and *-11* in *Arabidopsis*. *AtGH3-11 (JAR1/FIN219)* has been reported to adenylate jasmonic acid (JA) (Staswick *et al*. 2002), while *AtGH3-10* function is unknown. This study showed that *OsGH3-5* is involved in auxin response (Fig. 6d,e). Auxin responses play an important role in plant growth and development by forming local

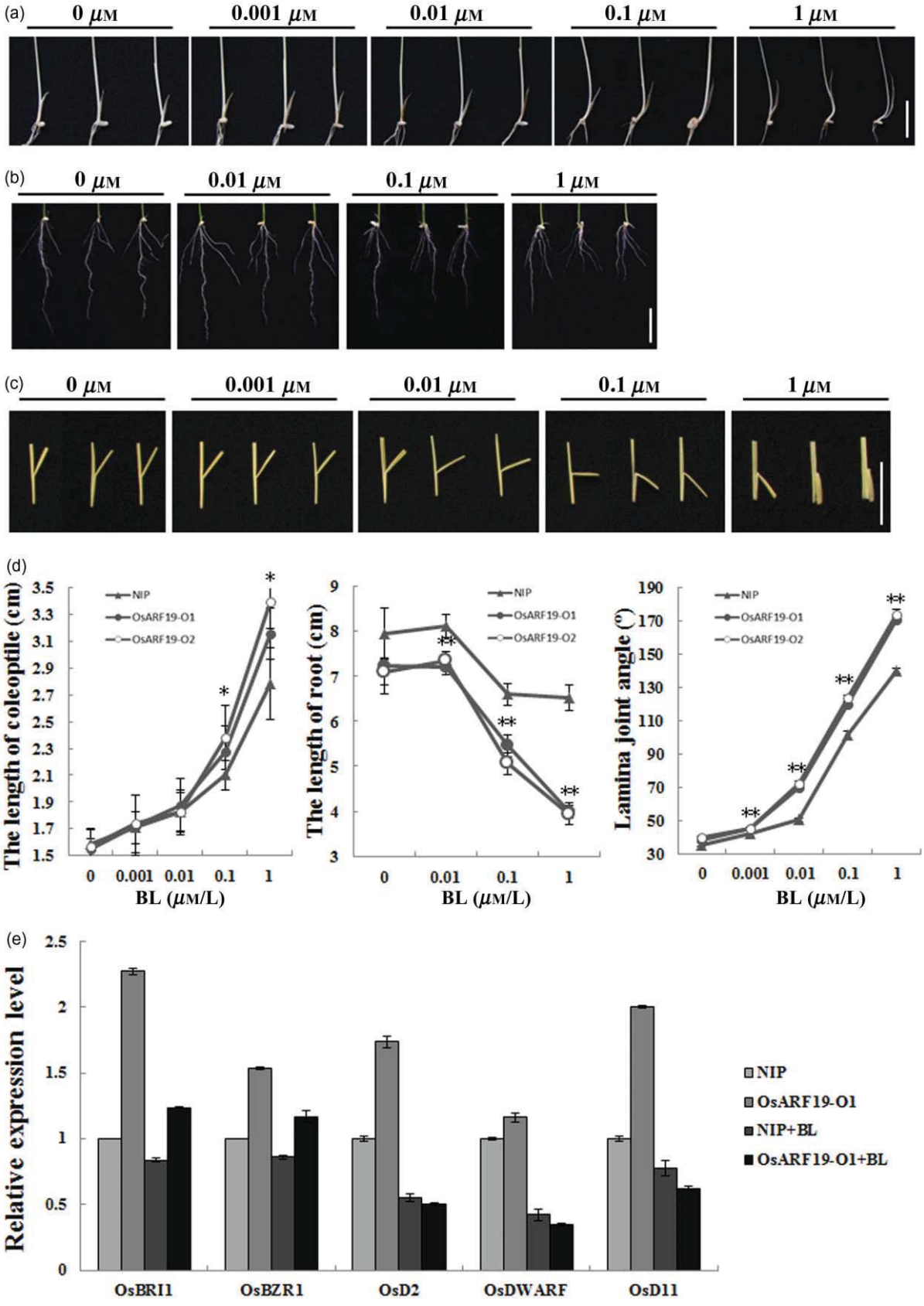

Figure 8. Morphological response of *OsARF19-O1* and *-O2* to 24-epibrassinolide (24-eBL). (a) Coleoptile elongation response to 24-eBL treatments. Panels from left to right show coleoptiles of 7 d seedlings of WT/NIP, *OsARF19-O1* and *OsARF19-O2* grown in the presence of 0, 0.001, 0.01, 0.1 and 1 μM 24-eBL under dark condition, respectively. Bar = 2 cm. (b) Primary root (PR) response to 24-eBL treatments. Panels from left to right show roots of 7 d seedlings of WT/NIP, *OsARF19-O1* and *OsARF19-O2* grown in the presence of 0, 0.01, 0.1 and 1 μM 24-eBL, respectively. Bar = 2 cm. (c) Leaf angle of response to 24-eBL treatments. Panels from left to right show each 2 cm lamina joints from top to bottom of 8 d seedlings of WT/NIP, *OsARF19-O1* and *OsARF19-O2* grown in the presence of 0, 0.001, 0.01, 0.1 and 1 μM 24-eBL for 3 d under dark condition, respectively. Bar = 2 cm. (d) Statistical analyses of coleoptile, PR lengths and lamina joint angles in WT/NIP, *OsARF19-O1* and *OsARF19-O2* under above indicated 24-eBL treatments. Ten rice lines were measured for each treatment. Bars indicate standard deviation ($n = 10$). * indicates significant difference at $P < 0.05$ and ** indicates $P < 0.01$. (e) Comparison of the expression of genes related to leaf angle in BR signalling among WT/NIP, *OsARF19-O1* and *OsARF19-O2*.

concentration gradients. As shown in Figs 6f,g and 7a,b, we found that free auxin levels at lamina joint of *OsGH3-5* and *OsARF19*-overexpression lines were significantly reduced, suggesting that lowering auxin contents might alter lamina inclination. Particularly, free auxin contents in *OsARF19-O1* were significantly decreased (Fig. 7a,b), implying that OsARF19 directs *OsGH3-1*, *-2*, *-5* and *-13* expressions resulting in an increase of auxin conjugates. These results are in agreement with those employing overexpression of *OsGH3-1*, -2 or *-13*, which showed significant reductions of free IAA levels, and caused morphological aberrations related to IAA deficiency, such as enlarged leaf angles (Zhang *et al*. 2009b; Du *et al*. 2012; Zhao *et al*. 2013).

OsARF19 regulates BR signalling through *OsBRI1*

In previous reports, the AuxRE, TGTCTC, was shown to act as a crosstalk point for BR and auxin signalling: ARFs target the AuxRE to regulate the expression of auxin response genes and BR response genes for controlling plant growth and development (Ulmasov *et al*. 1997a,b; Goda *et al*. 2002; Nakamura *et al*. 2003; Nemhauser *et al*. 2004; Walcher & Nemhauser 2012). Auxin and BR signalling share several genes, which are involved in plant growth and development-related processes (Vert *et al*. 2008). In *Arabidopsis*, both ARF2 and ARF7 were demonstrated to be involved in auxin–BR interaction through diverse ways (Vert *et al*. 2008; Zhou *et al*. 2013). In rice, OsARF11 targets the AuxRE of the promoter of the BR receptor kinase gene, *OsBRI1*, suggesting that ARF11 can control the degree of BR perception (Sakamoto *et al*. 2013). OsARF19 and OsARF11 have a close relationship in an evolutionary tree, belonging both to the class II subfamily of OsARF gene family in rice (Wang *et al*. 2007; Shen *et al*. 2010). Furthermore, *OsARF19-O1* is sensitive to BR treatments, and has a phenotype revealing increased leaf angles (Figs 1 & 8), which was opposite to the *osarf11*-Tos17 insertion mutant (Sakamoto *et al*. 2013). We show that OsARF19 directly binds to the *OsBRI1* promoter and controls the expression of *OsBRI1* (Supporting Information Fig. S7). These data suggest that OsARF19 functions as a bridge linking auxin and BR signalling during regulation of lamina inclination.

OsARF19 links to both auxin and BR signalling

Although several mutants revealing increased leaf angles have been reported, the molecular mechanism remained to be revealed, especially in respect to the molecular crosstalk between auxin and BR signalling. Here, we summarize that both pathways – *OsARF19-OsGH3-5* and *OsARF19-OsBRI1* – are involved in regulating leaf inclination (Fig. 9). In the *OsARF19-OsGH3-5* pathway, miR393 negatively regulates expression of *OsTIR1*, and OsTIR1 interacts with the OsIAA1 proteins (Bian *et al*. 2012); OsIAA1 also interacts with OsARF19 (Shen *et al*. 2010), which binds to the *OsGH3-5* promoter, positively regulating *OsGH3-5*. Finally, *OsGH3-5* overexpression impairs auxin response and reduces free auxin contents in the lamina joint (Fig. 6). In the *OsARF19-OsBRI1* pathway, OsARF19 binds to the *OsBRI1* promoter, positively regulating *OsBRI1* to activate a BR signal transduction pathway, which regulates the expression of the related gene *OsBZR1* and its downstream genes (Zhu *et al*. 2013) to affect lamina inclination. Therefore, apparently both described above co-modulate plant architecture, suggesting that the regulatory mechanism of the rice leaf angle might be more complicated than thought. Noteworthy, *OsARF23(1)* also interacts with OsIAA1 and antisense-*OsARF23(1)* line showed similar phenotype with *OsARF19-O1* (Attia *et al*. 2009; Song *et al*. 2009). Whether *OsARF23(1)* also binds to *OsGH3-5* as well as to *OsARF19*, and negatively regulates their expression during control of leaf angle, needs to be further investigated in the future.

Taken together, our physiological experiments, genetic analysis, cellular biological observation and molecular biological evidence support the finding that OsARF19 functions in bridging the molecular network of auxin and BR signalling. Moreover, underlying mechanisms might turn out to be useful for engineering rice architecture to culture high rice yield. In high-density plantings, characteristic semi-dwarf phenotype with erect leaves and shorter panicles was an ideal phenotype to improve grain yield (Morinaka *et al*. 2006; Sakamoto *et al*. 2006; Wu *et al*. 2008). *osarf19/osgh3-5* double mutant and *osgh3-5/osgh3-1* or *-2* or *-13* double or multiple

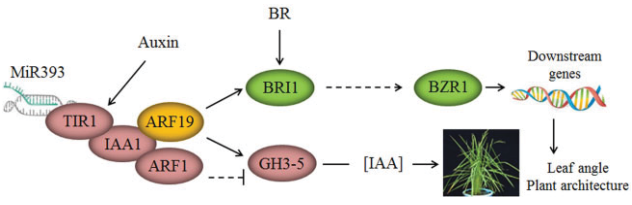

Figure 9. A proposed model for the role of OsARF19 in the regulation of rice leaf angle. ↓ and⊥ indicate positive and negative modes of regulation; [IAA] indicates auxin concentration.

mutants might be expected to create erected leaves. Further, identification of other downstream genes of *OsARF19* found in the ChIP assay would be essential for understanding the network regulating leaf inclination. In addition, auxin action in controlling leaf angle requires the BR signalling pathway, and vice versa, indicating that the roles of auxin and BR are interdependent. Furthermore, we show that auxin acts upstream of the major regulator of leaf angle size, *OsBRI1*, by recruiting the OsARF19 to control its expression. Our study uncovers a previously unknown regulatory factor of leaf angle size and a coordinating network of auxin and BR signalling in leaf angle regulation. These findings might be useful for optimal rice architectures.

ACKNOWLEDGMENTS

This project was funded by grants from the National Natural Science Foundation of China (31271692, 31171462 and 31371591), the National Science and Technology Support Plan (2012BAC09B01), the Natural Science Foundation for Distinguished Young Scholars of Zhejiang Province, China (LR13C130002) and the Swiss National Funds (to M.G.). We gratefully acknowledge Gynheung An in PFG (Plant Functional Genomics Laboratory), Korea, for contributing the T-DNA insertion mutant *osarf19*, and Akio Miyao in the RGRC (Rice Genome Resource Center), Japan, for providing the full-length cDNA clones of *OsARF19* and *OsGH3-5*, and *osgh3-5-TOS17* mutant, and Hongwu Bian for contributing *OsMiRNA393*-overexpression and *OsTIR1–RNAi* lines.

REFERENCES

Attia K.A., Abdelkhalik A.F., Ammar M.H., Wei C., Yang J., Lightfoot D.A., . . . El-Shemy H.A. (2009) Antisense phenotypes reveal a functional expression of OsARF1, an auxin response factor, in transgenic rice. *Current Issues in Molecular Biology* **1,** i29–i34.

Bai M.Y., Zhang L.Y., Gampala S.S., Zhu S.W., Song W.Y., Chong K. & Wang Z.Y. (2007) Functions of OsBZR1 and 14-3-3 proteins in brassinosteroid signaling in rice. *Proceedings of the National Academy of Sciences of the United States of America* **104,** 13839–13844.

Bian H., Xie Y., Guo F., Han N., Ma S., Zeng Z., . . . Zhu M. (2012) Distinctive expression patterns and roles of the miRNA393/TIR1 homolog module in regulating flag leaf inclination and primary and crown root growth in rice (*Oryza sativa*). *The New Phytologist* **196,** 149–161.

Cao H. & Chen S. (1995) Brassinosteroid-induced rice lamina joint inclination and its relation to indole-3-acetic acid and ethylene. *Plant Growth Regulation* **16,** 189–196.

Chen H., Zou Y., Shang Y., Lin H., Wang Y., Cai R., . . . Zhou J.M. (2008) Firefly-luciferase complementation imaging assay for protein–protein interactions in plants. *Plant Physiology* **146,** 368–376.

Chen J., Liu Y., Ni J., Wang Y., Bai Y., Shi J., . . . Wu P. (2011) OsPHF1 regulates the plasma membrane localization of low-and high-affinity inorganic phosphate transporters and determines inorganic phosphate uptake and translocation in rice. *Plant Physiology* **157,** 269–278.

Chen L., Xiong G., Cui X., Yan M., Xu T., Qian Q., . . . Wang Y. (2013) OsGRAS19 may be a novel component involved in the brassinosteroid signaling pathway in rice. *Molecular Plant* **6,** 988–991.

Cheng L., Wang F., Shou H., Huang F., Zheng L., He F., . . . Wu P. (2007) Mutation in nicotianamine aminotransferase stimulated the Fe(II) acquisition system and led to iron accumulation in rice. *Plant Physiology* **145,** 1647–1657.

Davies P. (1995) *Plant Hormones: Physiology, Biochemistry and Molecular Biology*, **Vol. 2,** Kluwer Academic Publishers, Dordrecht, the Netherlands.

Du H., Wu N., Fu J., Wang S., Li X., Xiao J. & Xiong L. (2012) A GH3 family member, OsGH3-2, modulates auxin and abscisic acid levels and differentially affects drought and cold tolerance in rice. *Journal of Experimental Botany* **63,** 6467–6480.

Du L., Ali G.S., Simons K.A., Hou J., Yang T., Reddy A.S. & Poovaiah B.W. (2009) Ca(2+)/calmodulin regulates salicylic-acid-mediated plant immunity. *Nature* **457,** 1154–1158.

Duan K., Li L., Hu P., Xu S.P., Xu Z.H. & Xue H.W. (2006) A brassinolide-suppressed rice MADS-box transcription factor, OsMDP1, has a negative regulatory role in BR signaling. *The Plant Journal: For Cell and Molecular Biology* **47,** 519–531.

Fan M., Xu C., Xu K. & Hu Y. (2012) Lateral organ boundaries domain transcription factors direct callus formation in *Arabidopsis* regeneration. *Cell Research* **22,** 1169–1180.

Garrett J.J., Meents M.J., Blackshaw M.T., Blackshaw L.C., Hou H., Styranko D.M., . . . Schultz E.A. (2012) A novel, semi-dominant ′allele of MONOPTEROS provides insight into leaf initiation and vein pattern formation. *Planta* **236,** 297–312.

Goda H., Shimada Y., Asami T., Fujioka S. & Yoshida S. (2002) Microarray analysis of brassinosteroid-regulated genes in *Arabidopsis*. *Plant Physiology* **130,** 1319–1334.

Hagen G. & Guilfoyle T.J. (1985) Rapid induction of selective transcription by auxins. *Molecular and Cellular Biology* **5,** 1197–1203.

Hiei Y., Ohta S., Komari T. & Kumashiro T. (1994) Efficient transformation of rice (*Oryza sativa* L.) mediated by *Agrobacterium* and sequence analysis of the boundaries of the T-DNA. *The Plant Journal: For Cell and Molecular Biology* **6,** 271–282.

Hong Z., Ueguchi-Tanaka M., Shimizu-Sato S., Inukai Y., Fujioka S., Shimada Y., . . . Matsuoka M. (2002) Loss-of-function of a rice brassinosteroid biosynthetic enzyme, C-6 oxidase, prevents the organized arrangement and polar elongation of cells in the leaves and stem. *The Plant Journal: For Cell and Molecular Biology* **32,** 495–508.

Hong Z., Ueguchi-Tanaka M., Umemura K., Uozu S., Fujioka S., Takatsuto S., . . . Matsuoka M. (2003) A rice brassinosteroid-deficient mutant, ebisu dwarf (d2), is caused by a loss of function of a new member of cytochrome P450. *The Plant Cell* **15,** 2900–2910.

Inukai Y., Sakamoto T., Ueguchi-Tanaka M., Shibata Y., Gomi K., Umemura I., . . . Matsuoka M. (2005) Crown rootless1, which is essential for crown root formation in rice, is a target of an AUXIN RESPONSE FACTOR in auxin signaling. *The Plant Cell* **17,** 1387–1396.

Jain M., Kaur N., Tyagi A.K. & Khurana J.P. (2006) The auxin-responsive GH3 gene family in rice (*Oryza sativa*). *Functional and Integrative Genomics* **6,** 36–46.

Ljung K., Hull A.K., Celenza J., Yamada M., Estelle M., Normanly J. & Sandberg G. (2005) Sites and regulation of auxin biosynthesis in *Arabidopsis* roots. *The Plant Cell* **17,** 1090–1104.

Mallory A.C., Bartel D.P. & Bartel B. (2005) MicroRNA-directed regulation of *Arabidopsis* AUXIN RESPONSE FACTOR17 is essential for proper development and modulates expression of early auxin response genes. *The Plant Cell* **17,** 1360–1375.

Morinaka Y., Sakamoto T., Inukai Y., Agetsuma M., Kitano H., Ashikari M. & Matsuoka M. (2006) Morphological alteration caused by brassinosteroid insensitivity increases the biomass and grain production of rice. *Plant Physiology* **141,** 924–931.

Mravec J., Skůpa P., Bailly A., Hoyerová K., Krecek P., Bielach A., . . . Friml J. (2009) Subcellular homeostasis of phytohormone auxin is mediated by the ER-localized PIN5 transporter. *Nature* **459,** 1136–1140.

Nakamura A., Higuchi K., Goda H., Fujiwara M.T., Sawa S., Koshiba T., . . . Yoshida S. (2003) Brassinolide induces IAA5, IAA19, and DR5, a synthetic auxin response element in *Arabidopsis*, implying a cross talk point of brassinosteroid and auxin signaling. *Plant Physiology* **133,** 1843–1853.

Nemhauser J., Mockier T.C. & Chory J. (2004) Interdependency of brassinosteroid and auxin signaling in *Arabidopsis*. *PLoS Biology* **2,** 1460–1471.

Ning J., Zhang B., Wang N., Zhou Y. & Xiong L. (2011) Increased leaf angle1, a Raf-like MAPKKK that interacts with a nuclear protein family, regulates mechanical tissue formation in the lamina joint of rice. *The Plant Cell* **23,** 4334–4347.

Okushima Y., Overvoorde P.J., Arima K., Alonso J.M., Chan A., Chang C., . . . Theologis A. (2005) Functional genomic analysis of the AUXIN RESPONSE FACTOR gene family members in *Arabidopsis thaliana*: unique and overlapping functions of ARF7 and ARF19. *The Plant Cell* **17,** 444–463.

Okushima Y., Fukaki H., Onoda M., Theologis A. & Tasaka M. (2007) ARF7 and ARF19 regulate lateral root formation via direct activation of LBD/ASL genes in *Arabidopsis*. *The Plant Cell* **19,** 118–130.

Qi Y., Wang S., Shen C., Zhang S., Chen Y., Xu Y. & Jiang D. (2012) OsARF12, a transcription activator on auxin response gene, regulates root elongation and affects iron accumulation in rice (*Oryza sativa*). *The New Phytologist* **193,** 109–120.

Qiao M., Zhao Z., Song Y., Liu Z., Cao L., Yu Y., . . . Xiang F. (2012) Proper regeneration from in vitro cultured *Arabidopsis thaliana* requires the microRNA-directed action of an auxin response factor. *The Plant Journal: For Cell and Molecular Biology* **71,** 14–22.

Sakamoto T., Morinaka Y., Ohnishi T., Sunohara H., Fujioka S., Ueguchi-Tanaka M., . . . Matsuoka M. (2006) Erect leaves caused by brassinosteroid deficiency increase biomass production and grain yield in rice. *Nature Biotechnology* **24,** 105–109.

Sakamoto T., Morinaka Y., Inukai Y., Kitano H. & Fujioka S. (2013) Auxin signal transcription factor regulates expression of brassinosteroid receptor gene in rice. *The Plant Journal: For Cell and Molecular Biology* **73,** 676–688.

Shen C., Wang S., Bai Y., Wu Y., Zhang S., Chen M., . . . Qi Y. (2010) Functional analysis of the structural domain of ARF proteins in rice (*Oryza sativa* L.). *Journal of Experimental Botany* **61,** 3971–3981.

Shen C., Wang S., Zhang S., Xu Y., Qian Q., Qi Y. & Jiang D.A. (2013) OsARF16, a transcription factor, is required for auxin and phosphate starvation response in rice (*Oryza sativa* L.). *Plant, Cell & Environment* **36,** 607–620.

Song Y., You J. & Xiong L. (2009) Characterization of OsIAA1 gene, a member of rice Aux/IAA family involved in auxin and brassinosteroid hormone responses and plant morphogenesis. *Plant Molecular Biology* **70,** 297–309.

Staswick P.E., Tiryaki I. & Rowe M.L. (2002) Jasmonate response locus JAR1 and several related *Arabidopsis* genes encode enzymes of the firefly luciferase superfamily that show activity on jasmonic, salicylic, and indole-3-acetic acids in an assay for adenylation. *The Plant Cell* **14,** 1405–1415.

Stowe-Evans E.L., Harper R.M., Motchoulski A.V. & Liscum E. (1998) NPH4, a conditional modulator of auxin-dependent differential growth responses in *Arabidopsis*. *Plant Physiology* **118,** 1265–1275.

Tabata R., Ikezaki M., Fujibe T., Aida M., Tian C.E., Ueno Y., . . . Ishiguro S. (2010) *Arabidopsis* auxin response factor6 and 8 regulate jasmonic acid biosynthesis and floral organ development via repression of class 1 KNOX genes. *Plant and Cell Physiology* **51,** 164–175.

Takase T., Nakazawa M., Ishikawa A., Kawashima M., Ichikawa T., Takahashi N., . . . Matsui M. (2004) Ydk1-D, an auxin responsive GH3 mutant that is involved in hypocotyl and root elongation. *The Plant Journal: For Cell and Molecular Biology* **37,** 471–483.

Tanabe S., Ashikari M., Fujioka S., Takatsuto S., Yoshida S., Yano M., . . . Iwasaki Y. (2005) A novel cytochrome P450 is implicated in brassinosteroid biosynthesis via the characterization of a rice dwarf mutant, dwarf11, with reduced seed length. *The Plant Cell* **17,** 776–790.

Tian C.E., Muto H., Higuchi K., Matamura T., Tatematsu K., Koshiba T. & Yamamoto K.T. (2004) Disruption and overexpression of auxin response factor 8 gene of *Arabidopsis* affect hypocotyl elongation and root growth habit, indicating its possible involvement in auxin homeostasis in light condition. *The Plant Journal: For Cell and Molecular Biology* **40,** 333–343.

Ulmasov T., Hagen G. & Guilfoyle T.J. (1997a) ARF1, a transcription factor that binds to auxin response elements. *Science* **276,** 1865–1868.

Ulmasov T., Murfett J., Hagen G. & Guilfoyle T.J. (1997b) Aux/IAA proteins repress expression of reporter genes containing natural and highly active synthetic auxin response elements. *The Plant Cell* **9,** 1963–1971.

Vert G., Walcher C.L., Chory J. & Nemhauser J.L. (2008) Integration of auxin and brassinosteroid pathways by Auxin Response Factor 2. *Proceedings of the National Academy of Sciences of the United States of America* **105,** 9829–9834.

Wada K., Marumo S., Ikekawa N., Morisaki M. & Mori K. (1981) Brassinolide and homobrassinolide promotion of lamina inclination of rice seedlings. *Plant and Cell Physiology* **22,** 323–325.

Walcher C.L. & Nemhauser J.L. (2012) Bipartite promoter element required for auxin response. *Plant Physiology* **158,** 273–282.

Waller F., Furuya M. & Nick P. (2002) OsARF1, an auxin response factor from rice, is auxin-regulated and classifies as a primary auxin responsive gene. *Plant Molecular Biology* **50,** 415–425.

Wang C., Ying S., Huang H., Li K., Wu P. & Shou H. (2009) Involvement of OsSPX1 in phosphate homeostasis in rice. *The Plant Journal: For Cell and Molecular Biology* **57,** 895–904.

Wang D., Pei K., Fu Y., Sun Z., Li S., Liu H. & Tao Y. (2007) Genome-wide analysis of the auxin response factor (ARF) gene family in rice (*Oryza sativa*). *Gene* **394,** 13–24.

Wang S., Bai Y., Shen C., Wu Y., Zhang S., Jiang D., . . . Qi Y. (2010) Auxin-related gene families in abiotic stress response in Sorghum bicolor. *Functional and Integrative Genomics* **10,** 533–546.

Wang S., Zhang S., Sun C., Xu Y., Chen Y., Yu C. & Qi Y. (2014) Auxin response factor (OsARF12), a novel regulator for phosphate homeostasis in rice (*Oryza sativa*). *The New Phytologist* **201,** 91–103.

Wilmoth J.C., Wang S., Tiwari S.B., Joshi A.D., Hagen G., Guilfoyle T.J., . . . Reed J.W. (2005) NPH4/ARF7 and ARF19 promote leaf expansion and auxin-induced lateral root formation. *The Plant Journal: For Cell and Molecular Biology* **43,** 118–130.

Wu C.Y., Trieu A., Radhakrishnan P., Kwok S.F., Harris S., Zhang K., . . . Pennell R.I. (2008) Brassinosteroids regulate grain filling in rice. *The Plant Cell* **20,** 2130–2145.

Wu X., Tang D., Li M., Wang K. & Cheng Z. (2013) Loose plant architecture 1, an indeterminate domain protein involved in shoot gravitropism, regulates plant architecture in rice. *Plant Physiology* **161,** 317–329.

Yamamuro C., Ihara Y., Wu X., Noguchi T., Fujioka S., Takatsuto S., . . . Matsuoka M. (2000) Loss of function of a rice brassinosteroid insensitive1 homolog prevents internode elongation and bending of the lamina joint. *The Plant Cell* **12,** 1591–1606.

Yang J.H., Han S.J., Yoon E.K. & Lee W.S. (2006) Evidence of an auxin signal pathway, microRNA167-ARF8-GH3, and its response to exogenous auxin in cultured rice cells. *Nucleic Acids Research* **34,** 1892–1899.

Yokota T. & Mori K. (1992) Molecular structure and biological activity of brassinolide and related brassinosteroids. In *Molecular Structure and Biological Activity of Steroids* (eds W.L. Duax & M. Bohl), pp. 317–340. CRC Press, Boca Raton, FL, USA.

Zhang C., Xu Y., Guo S., Zhu J., Huan Q., Liu H., . . . Chong K. (2012) Dynamics of brassinosteroid response modulated by negative regulator LIC in rice. *PLoS Genetics* **8,** e1002686.

Zhang L.Y., Bai M.Y., Wu J., Zhu J.Y., Wang H., Zhang Z., . . . Wang Z.Y. (2009a) Antagonistic HLH/bHLH transcription factors mediate brassinosteroid regulation of cell elongation and plant development in rice and *Arabidopsis*. *The Plant Cell* **21,** 3767–3780.

Zhang S.W., Li C.H., Cao J., Zhang Y.C., Zhang S.Q., Xia Y.F., . . . Sun Y. (2009b) Altered architecture and enhanced drought tolerance in rice via the down-regulation of indole-3-acetic acid by TLD1/OsGH3.13 activation. *Plant Physiology* **151,** 1889–1901.

Zhang Y., Su J., Duan S., Ao Y., Dai J., Liu J. & Wang H. (2011) A highly efficient rice green tissue protoplast system for transient gene expression and studying light/chloroplast-related processes. *Plant Methods* **7,** 30.

Zhao S.Q., Hu J., Guo L.B., Qian Q. & Xue H.W. (2010) Rice leaf inclination2, a VIN3-like protein, regulates leaf angle through modulating cell division of t the collar. *Cell Research* **20,** 935–947.

Zhao S.Q., Xiang J.J. & Xue H.W. (2013) Studies on the rice leaf inclination1 (LC1), an IAA-amido synthetase, reveal the effects of auxin in leaf inclination control. *Molecular Plant* **6,** 174–187.

Zhou X.Y., Song L. & Xue H.W. (2013) Brassinosteroids regulate the differential growth of *Arabidopsis* hypocotyls through auxin signaling components IAA19 and ARF7. *Molecular Plant* **6,** 887–904.

Zhu J.Y., Sae-Seaw J. & Wang Z.Y. (2013) Brassinosteroid signalling. *Development (Cambridge, England)* **140,** 1615–1620.

Received 18 April 2014; received in revised form 10 June 2014; accepted for publication 25 June 2014

SUPPORTING INFORMATION

Additional Supporting Information may be found in the online version of this article at the publisher's web-site:

Figure S1. Identification of *osraf19* mutant.
Figure S2. Analysis of AuxRE elements in promoters of *OsGH3* genes and *OsBRI1*.
Figure S3. Identification of *OsGH3-5*-overexpression lines.
Figure S4. Identification of the *osgh3-5* mutant.

Figure S5. Expression pattern of *OsGH3-5* in rice NIP.
Figure S6. *OsARF19* expression in *OsMiRNA393*-overexpression lines and *osafb2 (OsTIR1-RNAi)* mutant.
Figure S7. ChIP assay and yeast one hybrid of OsARF19 and *OsBRI1*.
Table S1. Statistical data of phenotypical characterization in WT/NIP, *OsARF19*-overexpression lines, WT/DJ and *osarf19*.
Table S2. Primer sequences for *OsARF19* gene.
Table S3. Primer sequences for OsGH3 genes.
Table S4. Primer sequences for ChIP-PCR analysis.
Table S5. Primer sequences for yeast one-hybrid assay.
Table S6. Primer sequences for co-expression analysis.
Table S7. Primer sequences for qRT-PCR analysis.